Available online at www.sciencedirect.com
SCIENCE DIRECT
Polymer 46 (2005) 1841–1850
polymer
www.elsevier.com/locate/polymer

Synthesis and thermal responsive properties of P(LA-*b*-EO-*b*-PO-*b*-EO-*b*-LA) block copolymers with short hydrophobic poly(lactic acid) (PLA) segments

X.Y. Xiong[a], K.C. Tam[a,*], L.H. Gan[b]

[a]*School of Mechanical and Production Engineering and Division of Chemical and Biomolecular Engineering, College of Engineering, Nanyang Technological University, Singapore 639798, Singapore*
[b]*Natural Sciences and Science Education, National Institute of Education, Singapore 637616, Singapore*

Received 31 October 2004
Available online 25 January 2005

Abstract

Poly(lactic acid) (PLA) was successfully grafted to both ends of Pluronic F87 block copolymer (PEO–PPO–PEO) to obtain amphiphilic P(LA-*b*-EO-*b*-PO-*b*-EO-*b*-LA) block copolymers (PLA–F87–PLA) with short PLA blocks. The block composition and structure of PLA–F87–PLA block copolymers were studied by nuclear magnetic resonance (NMR), gel permeation chromatography (GPC), differential scanning calorimetric (DSC) and wide angle X-ray diffraction (WXRD) techniques. The aggregation behavior of PLA–F87–PLA block copolymers in aqueous solutions was studied using the laser light scattering (LLS) technique. Various types of particles consisting of small micelles, medium and large aggregates were observed due to the complex structure of these copolymers. Importantly, PLA–F87–PLA block copolymers retain the thermal responsive behavior found in Pluronic systems. The critical micellization temperatures (CMTs) of PLA–F87–PLA were lower than that of F87 because of increased hydrophobicity introduced by the PLA blocks. A reversible sol–gel transition was observed for the hydrogels formed from PLA_6–F87–PLA_6 and PLA_9–F87–PLA_9 block copolymers. Preliminary results from the drug release study using a hydrophilic model drug procain hydrochloride (PrHy) were promising. Constant initial release rate was observed.

Keywords: Biocompatibility; Controlled drug release; Hydrogel

1. Introduction

Poly(ethylene oxide)–poly(propylene oxide)–poly (ethylene oxide) block copolymer (PEO–PPO–PEO) (commercially available as Pluronics) is a macromolecular surfactant that can aggregate into micelles in aqueous solution. The block polymer has been used widely as coating, foaming, detergent, solubilizing, thickening, and emulsifying agents [1]. Furthermore, the block copolymer has excellent biocompatibility and is one of the very few synthetic polymeric materials approved by the US Food and Drug Administration for use as food additives and pharmaceutical ingredients [2]. Hence, Pluronics are also potential candidates in biomedical applications such as drug delivery system, controlled release system and gene therapy [3–6].

The physical properties of Pluronics have been studied by several research groups [7–16]. Alexandridis et al. have published extensive reviews on the properties of Pluronics copolymers [1]. It is well-known that the micellization behavior of Pluronics varies with temperature depending on the composition and molecular weight. Pluronics also exhibit thermal-reversible gelation behavior. Pluronic F127 forms gel at the concentration greater than 18 wt%, indicating that high concentration is a necessary condition for gel formation. It was reported that no burst release was observed for drugs released from Pluronic gels and the loaded drug is

* Corresponding author.
E-mail address: mkctam@ntu.edu.sg (K.C. Tam).

0032-3861/$ - see front matter © 2005 Elsevier Ltd. All rights reserved.
doi:10.1016/j.polymer.2005.01.010

released initially at a constant rate [17–23]. This is an important factor for which Pluronic gel could be considered as attractive carriers for controlled drug release applications.

However, the critical micellization concentration (CMC) of Pluronic block copolymers is unacceptly high due to the weak hydrophobic PPO block. As a consequence, Pluronic micelles are generally not very stable, and this limits their potential applications as drug delivery systems. Hence, Pluronic copolymers have been modified with hydrophobic polyester blocks in order to impart good biocompatible and biodegradable properties. Ha et al. modified Pluronic copolymers with polycaprolactone (PCL) to obtain the block polymers PCL–Pluronic–PCL, which have very low CMC because of the high hydrophobic PCL blocks [24,25]. Yamaoka et al. [26] and our group [27] synthesized PLA–Pluronic–PLA block copolymers by attaching PLA blocks to both ends of Pluronic block copolymers. Although the CMC values of PCL–Pluronic–PCL and PLA–Pluronic–PLA are much smaller than Pluronics, the temperature-sensitivity of Pluronic block copolymers is lost because the PCL and PLA do not possess LCSTs.

In this study, we report the modifications of Pluronic F87 with short hydrophobic PLA blocks to produce PLA–F87–PLA block copolymers, which are highly soluble in water. More importantly, they retain the temperature-sensitive property of Pluronics. The aggregation and gelation behavior were studied in detail.

2. Experimental

2.1. Materials

Pluronic F87 were kindly supplied by BASF Corporation (Mount Olive, NJ, US) and dried overnight under vacuum before use. L-lactide was purchased from Aldrich and recrystallized from ethyl acetate (EtAc). The purified L-lactide was stored at 4–5 °C under argon environment. Stannous octoate ($Sn(Oct)_2$) was purchased from Aldrich and used as received. Model drug procaine hydrochloride (PrHy) were purchased from Aldrich and used as received.

2.2. Synthesis of PLA–F87–PLA block copolymers

Poly(lactic acid) (PLA) hydrophobic chains were attached to both ends of Pluronic F87 using stannous octoate ($Sn(Oct)_2$) as the catalyst to obtain amphiphilic block copolymers PLA–F87–PLA. A typical experimental procedure for the synthesis of a PLA–F87–PLA block copolymer designated as PLA_9–F87–PLA_9 is described as follows. A 100 ml round bottom flask with a stopcock was heated to remove the moisture under reduced pressure. After being cooled to room temperature, argon was introduced into the flask. Following this, L-lactide (18 mmol) and F87 (1.5 mmol) were added and heated to 100 °C with continuous stirring to produce a well-mixed molten phase. The mixture was then cooled, and $Sn(Oct)_2$ (0.1 wt% of L-lactide) was added to the flask under argon environment.

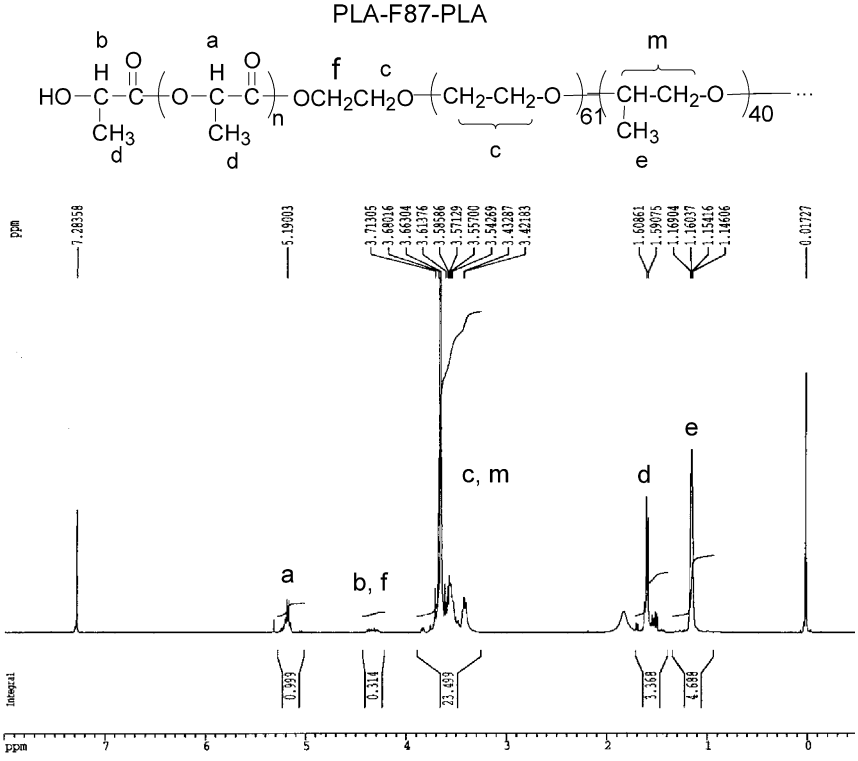

Fig. 1. ^1H NMR spectrum of PLA_{14}–F87–PLA_{14} ($CDCl_3$).

The vacuum-purge cycle was repeated for at least six times, and the mixture was degassed and heated to 180 °C. After stirring for 15 h, the reaction product was cooled to room temperature. The product was dissolved with methylene chloride, precipitated twice in 10-fold volume of methanol and once in 10-fold volume of diethyl ether. The polymer PLA_9–F87–PLA_9 was filtered and dried overnight under vacuum. A white powder with a yield of 80% was obtained. ^{1}H NMR (400 MHz, $CDCl_3$, TMS), δ (ppm): 1.15–1.17 (d, –OCH_2–CH(CH_3)–), 1.52–1.61 (m, –O–CH(CH_3)–CO–), 3.35–3.85 (m, –OCH_2–CH_2– and –OCH_2–CH(CH_3)–), 4.22–4.37 (m, HO–CH(CH_3)–CO– and –CO–OCH_2–CH_2–), 5.12–5.21 (m, –O–CH(CH_3)–CO) (Fig. 1). The other two block copolymers, assigned as PLA_6–F87–PLA_6 and PLA_{14}–F87–PLA_{14}, were similarly synthesized. In the nomenclature for the polymer 'PLA_6–F87–PLA_6, PLA_9–F87–PLA_9 and PLA_{14}–F87–PLA_{14}', the number '6, 9 and 14' corresponds to the number of repeat unit 'LA' in PLA–F87–PLA block copolymers, respectively.

3. Sample preparation

3.1. The preparation of PLA–F87–PLA aggregates in water

The PLA–F87–PLA aggregates in aqueous solutions were prepared as follows: a sample of PLA–F87–PLA block copolymer (10 mg) was first dissolved in 2 ml of tetrahydrofuran (THF), and the solution was then added drop-wise to 10 ml of distilled water with gentle stirring. THF was subsequently removed under reduced pressure and the concentration of the final solution is 0.1 wt%.

3.2. The preparation of PLA–F87–PLA hydrogels

The copolymers were first dissolved in acetone. A fixed amount of distilled water was added slowly into acetone solutions with gentle stirring. After this, acetone was removed under reduced pressure. The hydrogels formed from copolymers were equilibrated for 2 days.

3.3. In vitro drug release of PLA–F87–PLA hydrogels

A fixed amount of the copolymer and the model drug PrHy were first dissolved in acetone. A predetermined amount of distilled water was added slowly into the polymer solutions in acetone with gentle stirring and acetone was removed under reduced pressure. The drug loaded hydrogels were equilibrated for 2 days. A fixed amount of drug loaded hydrogel was introduced into a dialysis membrane (molecular weight cut-off, 8000 Da) and the sample was placed in a container filled with PBS solution. Then the container was placed in a shaking water bath at 37 °C for the drug release study. At different time intervals, 2 ml of the PBS solution outside the dialysis membrane was withdrawn and measured at wavelength 290 nm using ultra-violet spectrophotometer (HP UV, series 4). After the measurement, the solution was returned to the system.

3.4. Characterization

Nuclear magnetic resonance (NMR) spectra were recorded at room temperature using a Bruker ACF-400 (400 MHz) Fourier transform spectrometer. Chemical shifts (δ) were given in ppm using tetramethylsilane (TMS) as the internal reference. GPC of the copolymers was performed on an Agilent 1100 apparatus (Germany) equipped with a differential refractometer as the detector. Tetrahydrofuran (THF) was used as the mobile phase with a flow rate of 1.0 ml/min. Differential scanning calorimetric (DSC) thermograms were obtained using the modulated DSC 2920 (TA Instruments, Inc., New Castle, DE). The scanning rate was set at 10 °C/min. The sample (ca. 10 mg) was placed in an aluminum pan that was sealed using a sample pan crimper. The seal should be tight but not hermetic. The wide angle X-ray diffraction measurements (WXRD) were conducted using the Philips PW1830 powder diffractometer equipped with a Cu K_α radiation source. The X-ray diffractometer was operated at 20 kV and 10 mA. The CMT was measured using a Dataphysics DCAT-21 tensiometer. The rheological properties were studied by using a TA (Carrimed CSL 500) controlled stress rheometer, with a rough steel plate of 2 cm diameter. Silicon oil was applied around the sample and the plate to avoid evaporation of solvent.

4. Laser light scattering (LLS)

4.1. Static light scattering

Static light scattering (SLS) was used to measure and analyze the time-average scattered intensities. The method is often used to determine microscopic properties of particles such as the z-average radius of gyration (R_g), the weight-average molecular weight ($\bar{M}_w$) and the second virial coefficient (A_2) according to Eq. (1):

$$\frac{KC}{R_\theta} = \frac{1}{M_w}\left[1 + \frac{16\pi^2 n^2 \langle R_g^2\rangle \sin^2\left(\frac{\theta}{2}\right)}{3\lambda^2}\right] + 2A_2C \quad (1)$$

where, the Rayleigh ratio, $R_\theta = (I_s r^2/I_i \sin\theta)$; $K = [4\pi^2 n^2 (\partial n/\partial C)^2/(N_A \lambda^4)]$; C, the concentration of the polymer solution; n, the refractive index of the solvent; θ, the angle of measurement; λ, the wavelength of laser light; N_A, the Avogadro's constant and ($\partial n/\partial C$), the refractive index increment of the polymer solution. A plot of (KC/R_θ) versus [$\sin^2(\theta/2) + kC$] (where k is a plotting constant) can be used to determine the molecular parameters. By extrapolating the data to zero angle and concentration, R_g and A_2 can be obtained from the slopes, respectively. A simultaneous

Table 1
Characteristics of PLA–F87–PLA block copolymers

Sample	$\bar{M}_n$ (NMR)[a]	$\bar{M}_n$ (GPC)	$\bar{M}_w/\bar{M}_n$ (GPC)	$\bar{M}_w$[b]	Yield (%)
PLA_6–F87–PLA_6	8600	11,800	1.05	9000	73
PLA_9–F87–PLA_9	9000	12,400	1.05	9400	80
PLA_{14}–F87–PLA_{14}	9700	13,000	1.07	10,400	82

[a] Determined by the integration ratio of the peak at 1.58 ppm (–O–CH(CH_3)–CO–group in PLA block) and the peak at 1.15 ppm (–OCH_2–CH(CH_3)– group in Pluronic F87 block) in the ^{1}H NMR spectrum.
[b] $\bar{M}_w = \bar{M}_n$ (NMR)$\times[\bar{M}_w/\bar{M}_n$ (GPC)].

extrapolation to zero angle and concentration yields an intercept, which is the inverse of the $\bar{M}_w$.

4.2. Dynamic light scattering

The frequency of scattered light fluctuates around the incident light due to the constant motion of the polymer molecules. Dynamic light scattering (DLS) measures the intensity fluctuations with time and correlates these fluctuations to the properties of the scattering objects. In general, the terms of correlation functions of dynamic variables are always used to describe the response of the scattering molecules to the incident light. From the expression,

$$\Gamma = Dq^2 \tag{2}$$

the translational diffusion coefficients, D can be determined. Γ is the decay rate, which is the inverse of the relaxation time, τ, q the scattering vector ($q = (4\pi n \sin(\theta/2)/\lambda)$), where θ is the scattering angle, n is the refractive index of the solution, and λ is the wavelength of the incident light. If the Stokes–Einstein equation is used, the apparent hydrodynamic radius, R_h, can be calculated using the following equation:

$$R_h = \frac{kT}{6\pi\eta D} \tag{3}$$

where k, is the Boltzmann constant; T, the absolute temperature; η, the solvent viscosity.

A Brookhaven BIS200 laser scattering system was used to perform the static and dynamic light scattering experiments. The light source is a power adjustable vertically polarized 350 mW argon ion laser with a wavelength of 488 nm. The inverse Laplace transform of REPES supplied with the GENDIST software package was used to analyze the time correlation function (TCF), and the probability of reject was set to 0.5.

4.3. Transmission electron microscope (TEM)

TEM was performed on a JEOL JEM-2010 electron microscope at an acceleration voltage of 200 kV. The copper grid (400 meshes) with a carbon film was used. The copper grid was immersed in a drop of an aqueous polymer solution for 2 min, and then removed and dried. The sample was stained by two different methods. For the sample coated with osmium tetroxide, a drop of osmium tetroxide (OsO_4) in 2-methyl-2-propanol (2.5 wt%) was placed on the copper grid for 2 min. The copper grid was then dried overnight at room temperature prior to measurement. For the sample coated by platinum/palladium alloy, the copper grid was shadowed with the platinum/palladium alloy at a shadowing angle of ca. 33°.

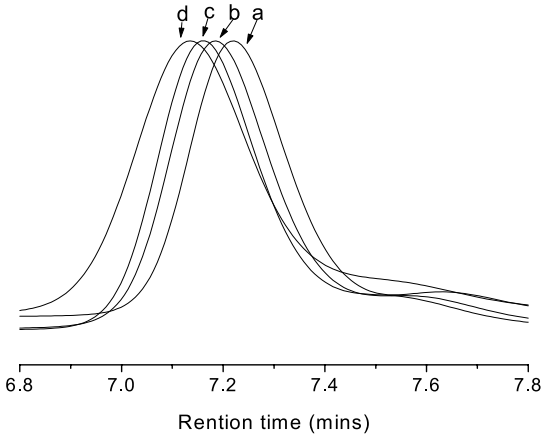

Fig. 2. GPC traces of (a) F87, (b) PLA_6–F87–PLA_6, (c) PLA_9–F87–PLA_9 and (d) PLA_{14}–F87–PLA_{14}.

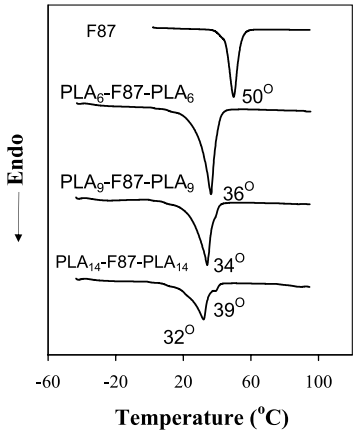

Fig. 3. The DSC results of PLA–F87–PLA block copolymers.

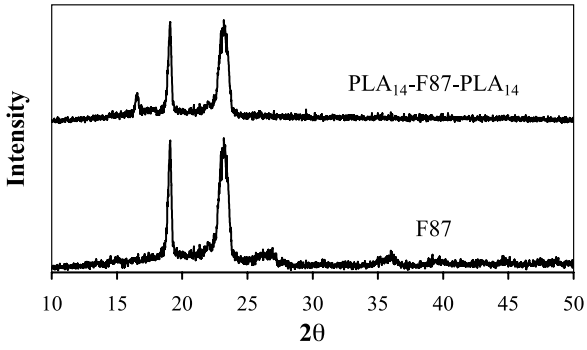

Fig. 4. The wide angle X-ray diffraction pattern of PLA_{14}–F87–PLA_{14} and F87 block copolymers.

5. Results and discussion

5.1. Synthesis and characterization

The block copolymers PLA–F87–PLA were synthesized by ring opening polymerization of the monomer L-lactide using Pluronic copolymer F87 as the initiator and stannous octoate ($Sn(Oct)_2$) as the catalyst via co-ordination polymerization mechanism [27,28]. The polymers were characterized by NMR and GPC techniques. Fig. 1 shows a ^1H NMR spectrum of PLA–F87–PLA in $CDCl_3$. The peak at ~4.30 ppm labelled 'b, f' consists of chemical shifts of the methylene protons of the PLA–CO–O*C*H_2–CH_2–O–F87– group and the methine proton of –F87–PLA–CO–C*H*(CH_3)–OH group since they overlapped. From the intensity ratio of the peak at 4.30 ppm (HO–C*H*(CH_3)–CO– and –CO–O*C*H_2–CH_2–) and the peak at 1.15 ppm (–OCH_2–CH(C*H*$_3$)–, the methyl protons of PPO block in F87), it was concluded that PLA blocks were attached to both ends of Pluronic F87. No homopolymer of PLA was formed as no peak was detected at 4.9–5.0 ppm, which belongs to the methine proton of the PLA–O–C*H*(CH_3)–COOH group [29].

The degree of polymerization ($\bar{DP}$, n) of PLA in PLA_n–F87–PLA_n copolymers was calculated from the peak intensity ratio of methyl protons of PLA (O–CH(C*H*$_3$)–CO–, 1.58 ppm) and methyl protons of F87 (–OCH_2–CH(C*H*$_3$)–, 1.15 ppm). The number-average molecular weight ($\bar{M}_n$) of the PLA_n–F87–PLA_n copolymer was obtained from the following expression:

$$\bar{M}_n = \bar{M}_n(F87) + 144n \quad (4)$$

The calculated molecular weight and molecular weight distribution of PLA in PLA_6–F87–PLA_6, PLA_9–F87–PLA_9 and PLA_{14}–F87–PLA_{14} block copolymers are showed in Table 1.

Fig. 2 shows the GPC traces of PLA–F87–PLA block copolymer and Pluronic F87. The molecular weight distribution ($\bar{M}_w/\bar{M}_n$) was determined by GPC (Table 1). The GPC results indicate that the block copolymers are pure as narrow and symmetrical single peaks were observed (Fig. 2).

5.2. Thermal properties

The DSC curves of PLA–F87–PLA block copolymers obtained at the second heating run are shown in Fig. 3. PLA_6–F87–PLA_6 and PLA_9–F87–PLA_9 exhibit only one endothermic peak whereas two endothermic peaks were observed for PLA_{14}–F87–PLA_{14}. The results indicate that PLA_{14}–F87–PLA_{14} consists of crystalline phase from both F87 and PLA blocks. This result is consistent with its X-ray diffraction pattern shown in Fig. 4. The two strong peaks at $2\theta = 19.1$ and 23.3° belong to the crystalline F87 and the small peak at $2\theta = 16.6°$ belongs to the crystalline PLA blocks. Apparently, the PLA blocks in PLA_{14}–F87–PLA_{14} are sufficiently long for the formation of crystalline phase.

Static and dynamic light scattering studies on the PLA–F87–PLA block copolymers in water were carried out. The concentration used in the laser light scattering experiments is equaled to or lower than 0.1 wt%, which is in the dilute

Table 2
Laser light scattering results of PLA–F87–PLA block copolymers in aqueous solutions at room temperature

Sample	R_h (nm)			R_g (nm)	$\bar{M}_w$ (aggregates)	$N_{aggregation}$ [a]
	Small	Middle	Large			
PLA_6–F87–PLA_6		160		226	7.2×10^6	800
PLA_9–F87–PLA_9	10	77	409	223	1.1×10^7	1200
PLA_{14}–F87–PLA_{14}	13	81		86	2.0×10^6	190

[a] $N_{aggregation} = \bar{M}_w$(aggregates)/$\bar{M}_w$(polymer), where $\bar{M}_w$ (polymer) is shown in Table 1.

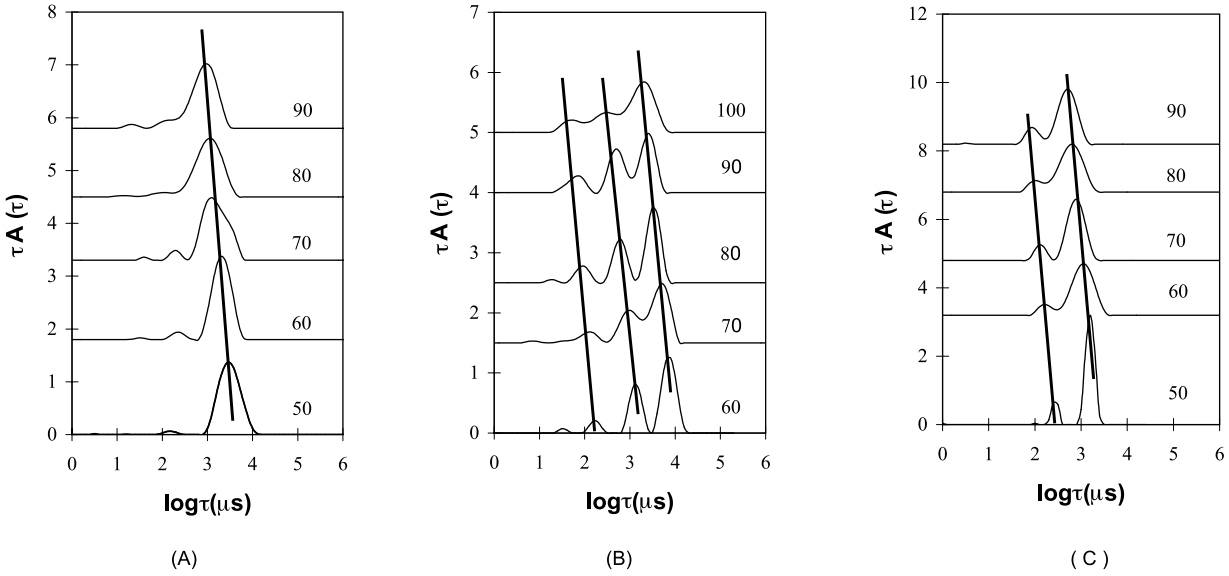

Fig. 5. Relaxation time distribution functions of PLA_6–F87–PLA_6 (*A*, 0.1 wt%), PLA_9–F87–PLA_9 (*B*, 0.1 wt%) and PLA_{14}–F87–PLA_{14} (*C*, 0.1 wt%) block copolymers in aqueous solutions at different scattering angles.

solution regime. The behavior of individual particles can be characterized under dilute solution concentrations [30].

The R_g, $\bar{M}_w$ and aggregation number ($N_{aggregation}$) of the three PLA–F87–PLA block copolymers were obtained from SLS measurements and are summarized in Table 2. It was found that R_g values decreased with increasing PLA block length.

The relaxation time distribution functions of PLA–F87–PLA block copolymers aqueous solutions at different scattering angles revealed only one major peak for PLA_6–F87–PLA_6, three peaks for PLA_9–F87–PLA_9 and two peaks for PLA_{14}–F87–PLA_{14} as shown in Fig. 5. The plots of Γ as a function of q^2 are shown in Fig. 6. Good q^2 dependency of Γ was observed for all the three block copolymers, indicating that the relaxation time peaks correspond to true particles. R_h values were calculated and are presented in Table 2. For some small peaks shown in Fig. 5(A) and (B), Γ are not dependent on q^2, indicating they do not correspond to true particles. They probably were arisen from the internal vibrational modes of the particles.

In order to confirm the coexistence of three kinds of particles for PLA_9–F87–PLA_9, the PLA_9–F87–PLA_9 sample was examined by TEM. The sample shown in Fig. 7(A) was stained with OsO_4. The real structure of large aggregates can be seen, but the contrast is not very good. In order to improve the contrast of TEM picture, PLA_9–F87–PLA_9 sample was also stained with platinum/palladium alloy as shown in Fig. 7(B). The small micelles with a diameter of around 20 nm were evident. The network-like complicated aggregates are observed in Fig. 7(A) and (B). The diameter of the large network-like aggregates varies from about 300 to 700 nm, which is consistent with that

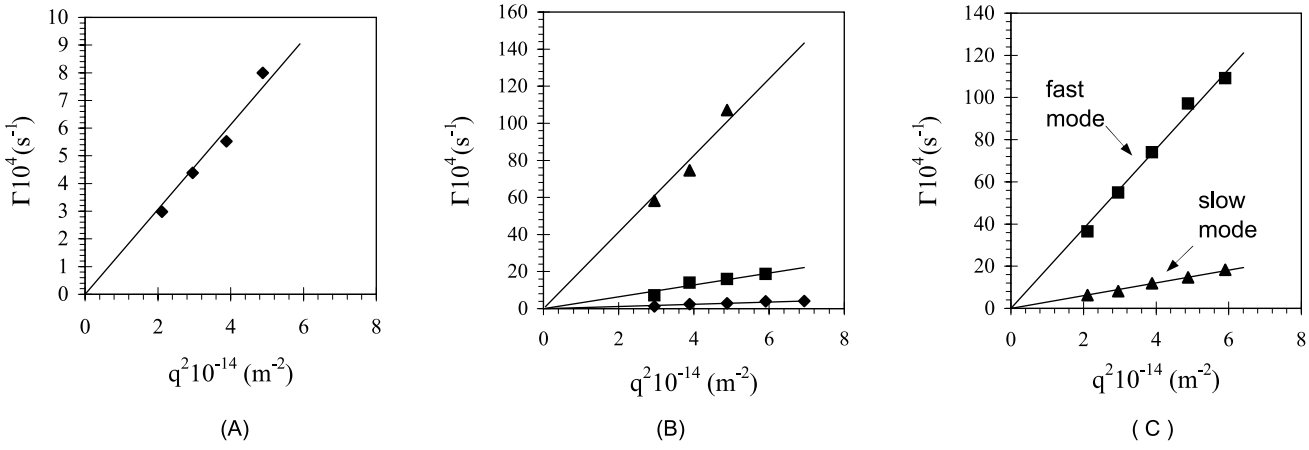

Fig. 6. Plots of *G* versus q^2 for PLA_6–F87–PLA_6 (*A*, 0.1 wt%), PLA_9–F87–PLA_9 (*B*, 0.1 wt%) and PLA_{14}–F87–PLA_{14} (*C*, 0.1 wt%) block copolymers in aqueous solution.

observed from DLS measurements. Therefore, several kinds of aggregates coexist for PLA–F87–PLA block copolymers in aqueous solution.

The aggregation behavior of PLA–F87–PLA with short PLA blocks was found to be rather complex compared to that of PLA–F127–PLA with long PLA blocks [27]. There is only one kind of nano-particles (R_h: 50–57 nm) observed for the latter [27]. However, there are two kinds of aggregates observed for PLA_{14}–F87–PLA_{14}, and three different aggregates for PLA_9–F87–PLA_9. These results indicate that the PLA block length in P(LA-*b*-EO-*b*-PO-*b*-EO-*b*-LA) block copolymers plays an important role in their aggregation behavior. P(LA-*b*-EO-*b*-PO-*b*-EO-*b*-LA) block copolymers consist of five blocks, two of which are hydrophilic PEO and three are hydrophobic PPO and PLA. For PLA–F87–PLA with short PLA blocks, although the hydrophobicity of PLA is stronger than PPO, the block length of PLA is much shorter than that of PPO. Thus the two hydrophobic PPO and PLA blocks could strongly influence the aggregation behavior, giving rise to the complex aggregation morphologies. However, the relatively simple aggregation behavior for PLA–F127–PLA with long PLA blocks should be due to the long and strongly hydrophobic PLA blocks.

In a comparative study, PLA_9–PEO_{182}–PLA_9 triblock copolymer ($\bar{M}_w/\bar{M}_n$ 1.06) with the same short PLA blocks was synthesized. The polymer was designed with the molar mass of PEO of 8000 g/mol similar to that of F87 ($\bar{M}_n$ 7700). The aggregation behavior of PLA_9–PEO_{182}–PLA_9 was again investigated by DLS at different scattering angles (50–100°). The relaxation time distribution function at 90° is shown in Fig. 8. Only one peak was observed and the R_h of aggregated particles was found to be 25 nm, indicating that the aggregation behavior of PLA_9–PEO_{182}–PLA_9 ($\bar{M}_n$, 9300 Da) is much simpler than that of PLA_9–F87–PLA_9 ($\bar{M}_n$, 9000 Da) block copolymer even though the chain length of PLA blocks is identical. Obviously, the presence of the PPO block in PLA_9–F87–PLA_9 has given rise to the observed complex aggregation behavior.

It is believed that the morphologies and particle size of aggregates formed from PLA–F87–PLA block copolymers should be related to the PLA block length since their aggregation behaviors are very different with different PLA block length. Further studies are needed to elucidate this factor.

The effect of concentration of PLA_{14}–F87–PLA_{14} aqueous solutions on the particle size was studied by dynamic light scattering (Fig. 9). The relaxation time peaks are invariable with changes in concentrations, indicating that the particle is not concentration dependent. This suggests that the aggregates of PLA_{14}–F87–PLA_{14} are produced via the closed association model.

5.3. Critical micellization temperature

The critical micellization temperature (CMT) of the three PLA–F87–PLA block copolymers in aqueous solutions was examined by surface tension measurement. No CMT was detected for PLA_{14}–F87–PLA_{14}. This indicates that PLA block length in PLA_{14}–F87–PLA_{14} is sufficiently long to negate the temperature-sensitive property of F87 block copolymer, which was confirmed by the DSC results. Both

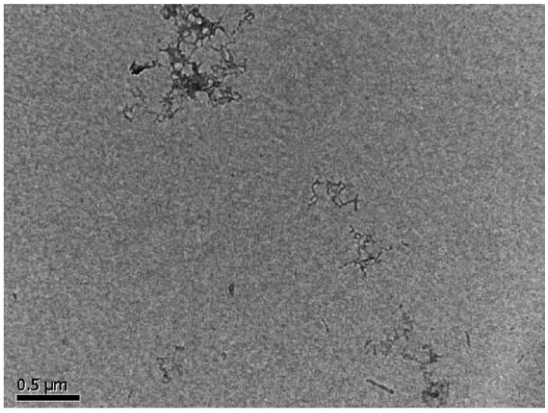

(A)

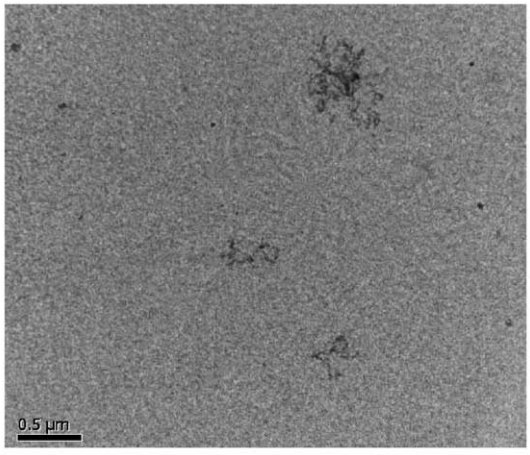

(B)

Fig. 7. TEM micrographs of aggregates formed from PLA_9–F87–PLA9 aqueous solution (0.15 wt%): (A) sample was stained with OsO_4; (B) sample was stained with platinum/palladium alloy.

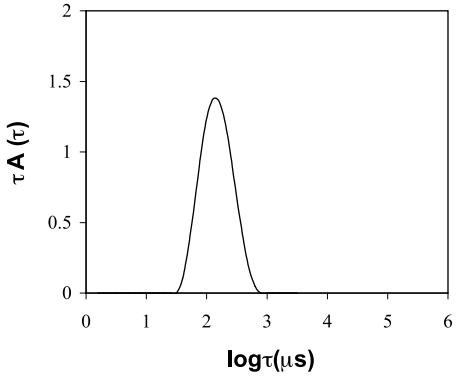

Fig. 8. Relaxation time distribution function of PLA_9–PEO_{182}–PLA_9 (0.1 wt%) in aqueous solutions at 90°.

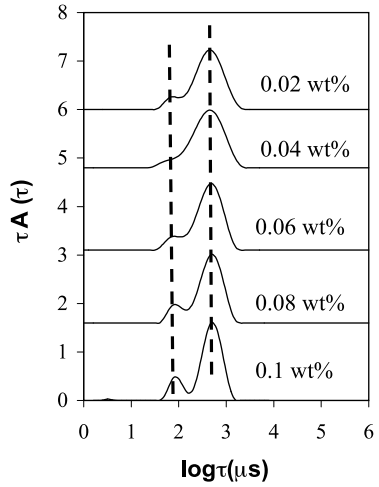

Fig. 9. Relaxation time distribution functions of PLA_{14}–F87–PLA_{14} in aqueous solutions with different concentrations at constant angle 90°.

PLA_6–F87–PLA_6 and PLA_9–F87–PLA_9 exhibit temperature-sensitive property showing CMT behavior. Fig. 10 shows the surface tension of PLA_6–F87–PLA_6 aqueous solutions as a function of temperature at different polymer concentrations. With increasing temperature, the solubility of polymer decreases, with more polymer chains partitioning onto the air–water interface. Hence, the surface tension decreases until the CMT is reached. After which, the surface tension should remain roughly constant due to the formation of polymeric micelles. However, as the surface tension of water decreases with increasing temperature, slight decreases of the surface tension with temperature above the CMT were observed as shown in Fig. 10. Similar plots of surface tension as a function of temperature at different polymer concentrations of PLA_9–F87–PLA_9 are shown in Fig. 11. For 2×10^{-4} wt% PLA_6–F87–PLA_6 and PLA_9–F87–PLA_9 aqueous solutions, the CMT are 42.1 and 40 °C, respectively. Comparing the CMC values of modified Pluronics (2×10^{-4} wt%) with F87 aqueous solution (0.5 wt%) at similar CMT of 41.7 °C [31], the CMCs of modified Pluronics are 2500 times lower than that of F87. The low CMC values are important consideration for the

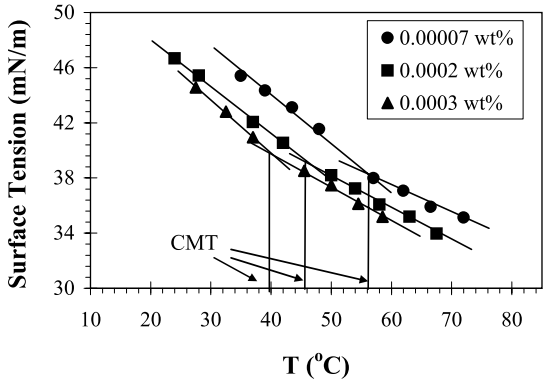

Fig. 10. Surface tension as a function of temperature for PLA_6–F87–PLA_6 block copolymer at different concentrations.

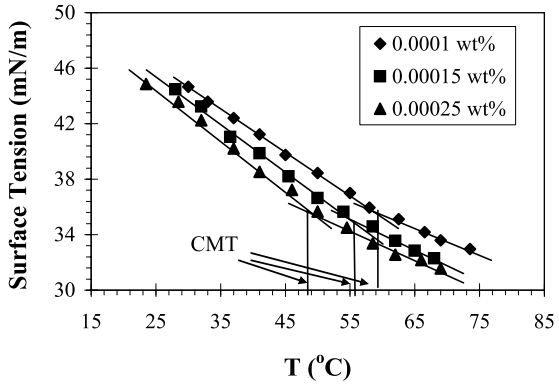

Fig. 11. Surface tension as a function of temperature for PLA_9–F87–PLA_9 block copolymer at different concentrations.

application in controlled release systems. The plots of CMT values as a function of polymer concentration for PLA_6–F87–PLA_6 and PLA_9–F87–PLA_9 block copolymers are shown in Fig. 12. For both polymers, the CMT decreases with increasing concentration due to the decrease in the polymer solubility, consistent with that of Pluronic block copolymers. Compared to Pluronic block copolymers [1], the temperature-sensitivity of PLA–F87–PLA block copolymers is much more dramatic. The CMT decreases much faster with increasing concentration, which is in agreement with that observed by Bromberg et al. [32].

5.4. Critical gelation temperature

The effect of temperature on the gelation properties of PLA–F87–PLA block copolymers was studied. Although there are various definitions of gel formation, it is generally agreed that a gel is formed when the storage molulus (G') is independent of angular frequency (ω), and when the storage modulus (G') is larger than the loss molulus (G'') [33–35]. For PLA–F87–PLA block copolymers, G', G'' were measured as a function of ω. Fig. 13 shows the plots of G' and G'' of PLA_9–F87–PLA_9 (40 wt%) block copolymers versus ω at 15 and 35 °C. At 15 °C, G' values were slightly lower than G'' and were dependent on ω, indicating that the

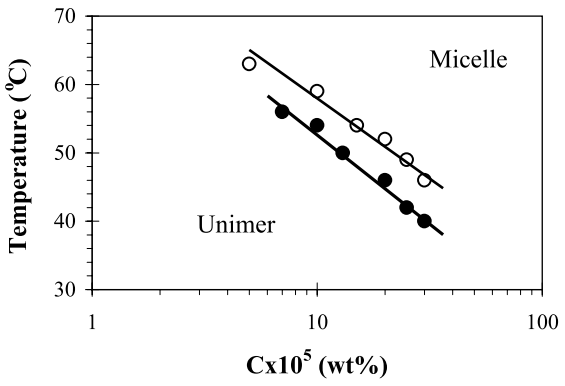

Fig. 12. The CMT–CMC boundary of PLA_6–F87–PLA_6 (●) and PLA_9–F87–PLA_9 (○) block copolymers.

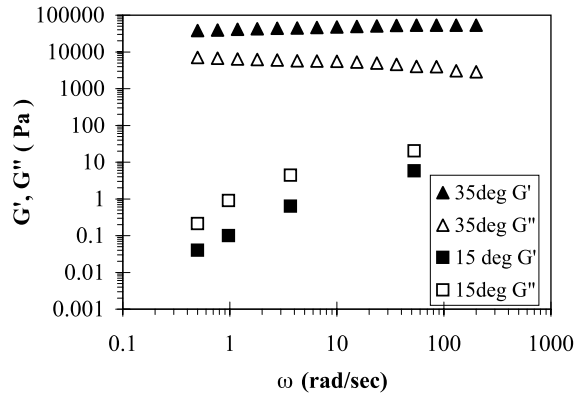

Fig. 13. G' and G'' of PLA_9–F87–PLA_9 (40 wt%) as a function of ω at 15 and 35 °C.

system was in the sol form. However, when the temperature was increased to 35 °C, G' increased by three orders of magnitude. In addition, G' values were larger than G'' and were almost independent of ω, indicating that a gel was formed.

The change of G' with temperature for PLA_9–F87–PLA_9 was also measured. The plots of G' as a function of temperature at different concentrations are shown in Fig. 14. The G' values increase by about 1000 times at the sol–gel transition. Excellent thermo-reversible sol–gel transition was demonstrated above a critical polymer concentration, similar to that observed for Pluronic block copolymers. PLA_6–F87–PLA_6 displayed similar phenomena. For PLA_{14}–F87–PLA_{14}, gel formation was observed above a critical polymer concentration, but its gelation behavior was not thermal-reversible. Apparently, Pluronic F87 lost its temperature-sensitive property when relatively longer hydrophobic chains were attached onto both ends, and this result is consistent with their temperature-sensitive behavior in aqueous solutions.

The plot of G' as a function of polymer concentration is shown in Fig. 15. The G' values of F87 and PLA–F87–PLA

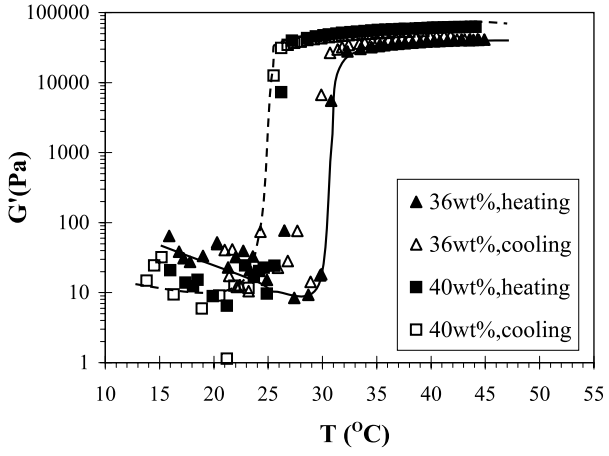

Fig. 14. G' of PLA_9–F87–PLA_9 as a function of temperature at different concentrations (36 and 40 wt%).

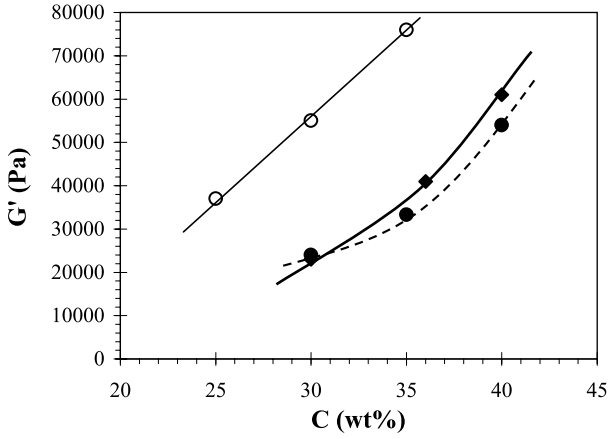

Fig. 15. G' of F87 (○), PLA_6–F87–PLA_6 (●) and PLA_9–F87–PLA_9 (♦) hydrogels as a function of concentration.

hydrogels increase with increasing concentration, indicating that PLA–F87–PLA hydrogels become stronger at high concentration. Fig. 16 shows the critical gelation temperature (CGT) values of PLA–F87–PLA hydrogels as a function of concentration. Compared with F87, the CGT values of PLA–F87–PLA hydrogels are higher when compared at the same polymer concentration. However, the hydrophobicity of PLA–F87–PLA hydrogels is larger than that of F87 gels, indicating that the former maybe able to deliver more hydrophobic drugs due to the presence of more hydrophobic PLA domains.

PLA–F87–PLA hydrogels could be used as carriers for both hydrophilic and hydrophobic drugs because they contain both hydrophilic and hydrophobic domains. The hydrophilic PrHy model drug was used to study the drug release behavior of PLA_6–F87–PLA_6 hydrogel in PBS (pH 7.4, 0.01 M) solution. The early stages of drug release were examined at two temperatures, 25 and 37 °C. The purpose to study the release process at different temperatures is to explore the effect of PLA_6–F87–PLA_6 thermo-reversible sol–gel transition on the release rate of the drug. The loaded hydrophilic model drug PrHy was found to increase the

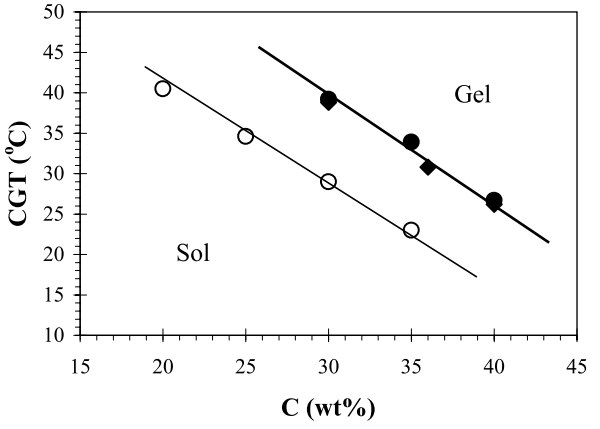

Fig. 16. CGT of F87 (○), PLA_6–F87–PLA_6 (●) and PLA_9–F87–PLA_9 (♦) hydrogels as a function of concentration.

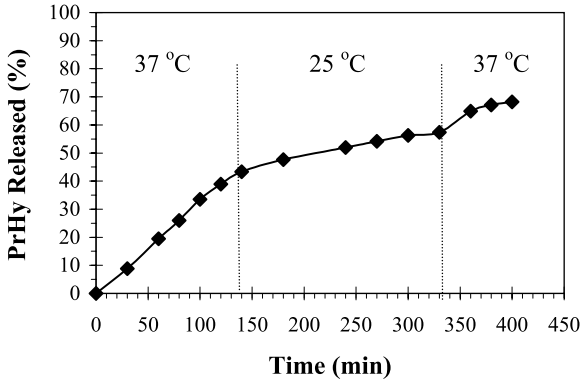

Fig. 17. The release behavior of PrHy (0.08 wt%) for loaded PLA_6–F87–PLA_6 (45 wt%) sample in PBS aqueous solutions at 25 and 37 °C.

CGT of PLA_6–F87–PLA_6 hydrogel. Ricci et al. also reported that the addition of hydrophilic drug may have an impact on the gel properties at the sol–gel transition, since the drug located outside the polymer micelles of gel can interfere with the gelation process [36]. The release behavior of PrHy (0.08 wt%) loaded in PLA_6–F87–PLA_6 (45 wt%) is shown in Fig. 17. PLA_6–F87–PLA_6 sample exists as a sol at 25 °C and a gel at 37 °C. Interestingly, no burst release was observed and PrHy was released from PLA_6–F87–PLA_6 sample at a constant rate at both 25 and 37 °C. We noted that the temperature has an effect on the release rate of PrHy, where PrHy is released faster from PLA_6–F87–PLA_6 gel at 37 °C than from its sol at 25 °C. Further study on the drug release kinetics of PLA–F87–PLA hydrogels is in progress.

6. Conclusions

PLA–F87–PLA block copolymers with short hydrophobic PLA chains were successful synthesized. The aggregation behavior of PLA–F87–PLA in aqueous solutions is complex because of rather complicated block structure. Various kinds of particles (micelles and large aggregates) were observed. Importantly, PLA–F87–PLA block copolymers retain the temperature-sensitive property of Pluronics. They were confirmed by CMT results from the surface tension and CGT from the rheological measurements. The initial constant release of hydrophilic model drug from PLA–F87–PLA hydrogel was observed.

Acknowledgements

We would like to acknowledge the financial support in the form of a SDS grant from the School of MPE. Xiong XY would like to thank NTU for the financial support in the form of a PhD graduate scholarship.

References

[1] Alexandridis P, Hatton TA. Colloids Surf 1995;96:1–46.
[2] Svingen R, Alexandridis P, Akerman B. Langmuir 2002;18:8616–9.
[3] Moghimi SM. Adv Drug Deliv Rev 1995;16:183–93.
[4] Kabanov AV, Lemieux P, Vinogradov S, Alakhov VY. Adv Drug Deliv Rev 2002;54:223–33.
[5] Kabanov AV, Batrakova EV, Alakhov VY. Adv Drug Deliv Rev 2002;54:759–79.
[6] Kabanov AV, Batrakova EV, Miller DW. Adv Drug Deliv Rev 2003;55:151–64.
[7] Bohorquez M, Koch D, Trygstad T, Pandit N. J Colloid Interface Sci 1999;216:34–40.
[8] Pandya K, Bahadur P, Nagar TN, Bahadur A. Colloid Surf A 1993;70:219–27.
[9] Linse P, Malmsten M. Macromolecules 1992;25:5434–9.
[10] Alexandridis P, Holzwarth JF, Hatton TA. Macromolecules 1994;27:2414–25.
[11] Su YL, Wang J, Liu HZ. Macromolecules 2002;35:6426–31.
[12] Su YL, Wang J, Liu HZ. Langmuir 2002;18:5370–4.
[13] Kositza MJ, Bohne C, Alexandridis P, Hatton TA, Holzwarth JF. Macromolecules 1999;32:5539–51.
[14] Mortensen K, Pedersen JS. Macromolecules 1993;34:805–12.
[15] Wanka G, Hoffmann H, Ulbricht W. Macromolecules 1994;27:4145–59.
[16] Goldmints I, von Gottberg FK, Smith KA, Hatton TA. Langmuir 1997;13:3659–64.
[17] Moore T, Croy S, Mallapragada S, Pandit N. J Control Release 2000;67:191–202.
[18] Anderson BC, Pandit NK, Mallapragada SK. J Control Release 2001;70:157–67.
[19] Alexandridis P, Zhou D, Khan A. Langmuir 1996;12:2690–700.
[20] Cau F, Lacelle S. Macromolecules 1996;29:170–8.
[21] Gilbert JC, Hadgraft J, Bye A, Brookes LG. Int J Pharm 1986;32:223–8.
[22] Pandit NK, Wang D. Int J Pharm 1998;167:183–9.
[23] Moore T, Croy S, Mallapragada S, Pandit N. J Control Release 2000;67:191–202.
[24] Ha JC, Kim SY, Lee YM. J Control Release 1999;62:381–92.
[25] Kim SY, Ha JC, Lee YM. J Control Release 2000;65:345–58.
[26] Yamaoka T, Takahashi Y, Fujisato T, Lee CW, Tsuji T, Ohta T, Murakami A, Kimura A. J Biomed Mater Res 2001;54:470–9.
[27] Xiong XY, Tam KC, Gan LH. Macromolecules 2003;36:9979–85.
[28] Kricheldorf HR, Krerser-saunders I, Boettcher C. Polymer 1995;35:219.
[29] Rashkov I, Manolova N, Li SM, Esplartero JL, Vert M. Macromolecules 1996;29:50–6.
[30] Dai S, Tam KC, Jenkins RD. Macromolecules 2000;33:7021–8.
[31] Beezer AE, Loh W, Mitchell JC, Royall PG, Smith DO, Tute MS, Armstrong JK, Chowdhry BZ, Leharne SA, Eagland D, Crowther NJ. Langmuir 1994;10:4001–6.
[32] Bromberg L, Temchenko M. Langmuir 1999;15:8633–9.
[33] Li L. Macromolecules 2002;35:5990–8.
[34] Winter HH, Chambon F. J Rheol 1986;30:367–82.
[35] Clark AH, Gidley MJ, Richardsib RK, Ross-Murphy SB. Macromolecules 1989;22:346–51.
[36] Ricci EJ, Bentley MVLB, Farah M, Bretas RESJ, Marchetti M. Eur J Pharm Sci 2002;17:161–7.